The Center for Particle Theory

THE UNIVERSITY OF TEXAS AT AUSTIN

Cluster Formulation in the Dual Topological Unitarization

by

Monowar Hossain

Center for Particle Theory
Department of Physics
The University of Texas at Austin
Austin, Texas 78712

Abstract

The work of Chiu, Hossain and Tow is generalized by incorporating the no double counting condition and the t_{min} effect in the integral equations for the Reggeon and the Pomeron. The relation between the no double counting condition and the average cluster separation is derived, and a test is proposed to determine the correct counting. It is shown that the t_{min} effect is quite important in determining the Regge parameters. The model predicts a relation between five physical quantities: the Pomeron intercept (α_p^0) and slope (α_p'), the magnitude (k) and the exponential dependence (b) of the triple-Regge vertex, and the ratio of Pomeron to Reggeon residues (c) at t = 0. The solutions obtained are well within the range of acceptable values. A reasonable solution is, for example, $\alpha_p^0 = .92$, $\alpha_p' = .2$, $b = 1.6$, $k = 12.9$ and $c = 0.91$. It is found that cuts are present in both the Reggeon and the Pomeron amplitudes, and their contributions are small compared to the leading poles.

I. INTRODUCTION

In the Dual Topological Unitarization (DTU) scheme,[1] all the planar diagrams in the unitarity sum generate the Reggeons. The next important set of diagrams has the topology of a cylinder, and their effect is to renormalize the Reggeon which has the vacuum quantum numbers. The tensor f-trajectory is renormalized upwards, and it is identified[2] with the Pomeron trajectory. In performing the unitarity sum it is usual[3-15] to assume that groups of hadrons (which are called clusters) are produced first, and then they decay into other particles. Experimental evidence[16] also supports this cluster picture. The contributions of different clusters are included by integrating over each cluster up to a certain maximum cluster size (say, $\bar{s}$), together with appropriate no double counting[9] (NDC) conditions.

A number of works[2-15] has been done in the DTU scheme up to the planar and the cylinder levels. However, most of them do not include the effects of NDC[6,7,10,11,12] or treat the t-dependence of the Reggeon loops approximately[2,5-15] (i.e., take only $t = 0$, or integrate over t by neglecting the t_{min} effect). Chan and his collaborators[3,4] have set up integral equations at planar and cylinder levels and have solved them. Their formulation has assumed NDC condition at the planar level, which allows smaller separation between different clusters, and, therefore, the assumption

of Regge exchange may not be good. We shall show later that the choice of NDC condition corresponds to a definite assumption about the production mechanism of the hadrons in the multiperipheral chain. Therefore, the correct NDC is determined by the dynamics of the cluster production (e.g., the cluster size and gap). In the previous works[3-5,7-9,15] the NDC has been assumed on an ad hoc basis, and its relation to the dynamical production mechanism was not determined.

The produced clusters in the multiperipheral chain can be heavy (up to $s \sim 5$ GeV^2). If s_1 and s_2 are the invariant (mass)^2 of the two neighboring clusters, then the minimum value of momentum transfer t_{min} is given by $-s_1 s_2/s_{12}$ [a more accurate expression is given in Eq. (16)]. In several works[2,6,9,10,14,15] the integration over t has been neglected. Even when the t integration is performed, in many previous works[5,7,8,11-13] t_{min} has been set euqal to zero. This may be a good approximation when the produced particles (s_1 or s_2) are light, e.g., pions. But when heavier particles like vector and tensor mesons are produced, t_{min} cannot be neglected. Chan et al.[3,4] have taken into account t_{min} in their works. However, it is clear from the above expression that the effect of t_{min} depends on the NDC used. As explained in section II, we shall use a different NDC in our work.

The purpose of this paper is twofold. Firstly, we investigate the connection between the NDC and the mechanism

of multiparticle production. We have outlined the calculation of the average gap between the clusters (in rapidity) if the cluster size and the rapidity distribution of the final particles are known. The gaps are calculated for the NDC's of Refs. 4 and 9, assuming that the produced particles are uncorrelated. We argue that the experimental determinations of the average gap will determine the correct counting. Secondly, the calculation in the DTU scheme is carried out up to the cylinder level by properly including the t_{min} effect and the NDC. This is a generalization of the work of Chiu, Hossain and Tow.[7] We set up the integral equations for the planar and the cylinder levels. By choosing a suitable parametrization for the triple-Reggeon vertex,[13] the integration over the phase space is performed. This automatically includes the effect of t_{min}. For NDC at the planar level, the prescription of Ref. 9 has been used. At the cylinder level, we have proposed a new NDC (see section III). We bootstrap the leading Reggeon and obtain the value of the triple-Regge vertex k for each value of the parameter b (which gives the exponential behaviour of the triple-Regge vertex). We then use the Pomeron equation to calculate the Pomeron intercept α_p^0, and the slope α_p'. The ratio of Pomeron to Reggeon residues at t = 0, c is also calculated from the Reggeon and Pomeron equations. This furnishes constraint relations for these five quantities

(b, k, α_p^0, α_p' and c).

The plan of the paper is as follows. In section II we discuss the double counting problem associated with the clusters. Reggeon and Pomeron integral equations are set up, and the conditions for Reggeon and Pomeron output poles and expressions for cuts are derived in section III. Numerical results are given in section IV, and in section V, the main conclusions are summarized. Some detail calculations are given in the appendices.

II. DOUBLE COUNTING PROBLEM

There is experimental evidence[16] that in the high energy scattering processes, clusters are produced independently. Each cluster then decays isotropically (in the cluster rest frame), independent of all others. Apart from some correlation between the particles from the same cluster, these decay products are distributed in an uncorrelated manner. However, in classifying an event in terms of clusters, ambiguities may arise due to overcounting or undercounting of the final state configurations. A given number of particles may be divided into two clusters in many ways. One should, therefore, have a unique way to define the cluster, so that all possible configurations are included once and only once. This prescription of no double counting (NDC) should also reproduce the correct separation (in rapidity) between the clusters. In the following, we shall assume that the distribution of the final particles which are detected is known. We then calculate the separation between two adjacent clusters in two models [the NDC prescriptions of Refs. 4 and 9].

We follow the work of Finkelstein and Koplik.[9] If the particles are produced at random on the rapidity axis, then the probability distribution of the interparticle spacings would be given by,[9,16]

$$\rho(\ell) = ae^{-\ell a} , \qquad (1)$$

where ℓ is the separation of the rapidities of the two particles, and 1/a is the average interparticle spacing. One can use the experimentally observed distribution function in place of Eq. (1). This may result in a quantitative change, but will not alter the general conclusions.

We now calculate the average separation between two adjacent clusters using the NDC of Ref. 9 (we call this model A). If there are two adjacent clusters of invariant $(\text{mass})^2$ s_1 and s_2, and s_{12} is the total $(\text{mass})^2$ of the system, then the NDC of model A is,

$$s_0 < s_1 < \bar{s} \tag{2a}$$

$$s_0 < s_2 < \text{minimum of } (\bar{s}, m_T^2 s_{12}/\bar{s}) \ . \tag{2b}$$

Here s_0 is the threshold $(\text{mass})^2$, and m_T^2 is the transverse mass squared of the produced particles. The upper limit of s_2 is motivated by the multiperipheral nature of the production processes. For simplicity, we will assume that $m_T^2 = s_0$ in our work. This assumption will not affect our general conclusions. In Fig. 1, this model is illustrated in the rapidity language. The particles 1, 2, 3 ... are arranged in order according to their rapidities. We start from particle 1, mark off a distance $\bar{L}$ $(= \ln\frac{\bar{s}}{s_0})$, and call this the first cluster. The next cluster spreads over a

distance $\bar{L}$ from the particle immediately to the right of the first cluster.

Suppose that x is the point where the first cluster terminates. Then the interval Δ_1 in which x lies is given by,[9]

$$\Delta_1 = \frac{1}{a} - \frac{\bar{L}}{e^{\bar{L}a} - 1} . \tag{3}$$

This may be interpreted as the average separation between two clusters.

The NDC prescription of Chan et al.[4] (model B) is defined as,

$$s_1, s_2 < \bar{s} \quad \text{and} \quad s_{12} > \bar{s} . \tag{4}$$

In this NDC (as we will see below), the average separation between the clusters is smaller. Therefore, their assumption of a multi-Regge amplitude is not very good. This model is illustrated in Fig. 2 in the rapidity language. Here,

$$L_1 \leq \bar{L}, \quad L_2 \leq \bar{L} \quad \text{and} \quad L_t > \bar{L} . \tag{5}$$

If d is the average distance between x and y, then one gets,

$$d(L') = \int_0^{L'} \ell\rho(\ell)d\ell \Big/ \left[\int_0^{L'} \rho(\ell)d\ell \right]$$

$$= \frac{1}{a} - \frac{L'}{e^{L'a} - 1} , \tag{6}$$

where $L' = L_t - L_1$. One has to average over the variables L_t and L_1 in order to get the average separation Δ_2. First note that,

$$L_2 - \bar{L} \leq 0 \ . \tag{7a}$$

We can rewrite this as,

$$L' - \bar{L} - d \leq 0 \ . \tag{7b}$$

Using Eq. (6), one can solve for the maximum value of L' from the above equation. We call this L'_{max}. Then the average gap Δ_2 is given by,

$$\Delta_2 = \frac{2}{L'^2_{max} - (L'_{max} - \bar{L})^2} \cdot \int_0^{\bar{L}} dL_1 \int_{\bar{L}-L_1}^{L'_{max}} dL' d(L') \ . \tag{7c}$$

Equations (3) and (7c) give the average separation between clusters in the two models. Taking, for example, $\bar{L} \approx 4/a$, we find that $\Delta_1 \approx 2/a$ and $\Delta_2 \approx 1/a$. These quantities can be compared with the experimental values. It may be noted that in model A, the average separation of the clusters is larger than the interparticle spacing $1/a$, whereas, in model B, it is nearly equal to $1/a$. When two clusters are very close, then the Regge exchange picture is not very appropriate. The NDC defined by equation (2) allows more gap (on the

average) between the clusters, and may be favored more from the Regge exchange assumption. We, therefore, follow this NDC in the next section.

III. THE INTEGRAL EQUATIONS FOR THE REGGEON AND THE POMERON

In this section, we develop a t-dependent bootstrap program up to the cylinder level by incorporating the NDC and the t_{min} effect. For simplicity, we have assumed that the SU(N) symmetry is exact.

Reggeon: The Reggeon amplitude $A_{P,ab}(s,t)$ (the subscript P stands for the planar diagram) has the integral equation[7] (see Fig. 3),

$$A_{P,ab}(s,t) = P_{0,ab}(s,t) + T_{P,ab}(s,t) , \qquad (8)$$

where $P_{0,ab}(s,t)$ is the inhomogeneous term, and $T_{P,ab}(s,t)$ is the homogeneous term. $T_{P,ab}$ is given by,

$$T_{P,ab}(s,t) = \int_{P.S.} P_{0,a2}(s_1,t) A_{P,2b}(s_2,t) z_2 , \qquad (9)$$

where $z_2 = \cos\pi(\alpha_2-\alpha_2')$, $\alpha_i = \alpha(t_i)$ and $\alpha_i' = \alpha(t_i')$. P.S. means the integration over the phase space (see Appendix A).

We now incorporate the NDC of Finkelstein and Koplik[9] in our phase space integration, Eq. (A-1). We take s_1 between s_0 and $\bar{s}$, and s_2 between s_0 and $s_0 s/\bar{s}$, for the Reggeon integral equation (see Eq. (2b)).

To simplify the notation, we remove the external vertices associated with the particles a and b, and rewrite Eq. (8) as,

$$A_p(s,t) = P_0(s,t) + T_p(s,t) \ . \qquad (10)$$

Writing out the triple-Regge vertex $g(t,t_2,t_2')$ explicitly, we get from Eq. (A-1),

$$T_p(s,t) = \frac{1}{8\pi^2} \int_{s_0}^{\bar{s}} ds_1 P_0(s_1,t) \int_{s_0}^{ss_0/\bar{s}} ds_2 A_p(s_2,t) \int dt_2 dt_2' \; z_2 g^2(t,t_2,t_2') \left(\frac{s}{s_1 s_2}\right)^{\alpha_2+\alpha_2'} \frac{\theta(-\Delta)}{|\Delta|^{1/2}} \ . \qquad (11)$$

Pomeron: The integral equation for the Pomeron is given by the sum of the planar and the cylinder diagrams. Diagrammatically, the integral equation for the Pomeron amplitude is represented in Fig. 4. The NDC for the uncrossed kernel is the same as before. The case of the crossed propagator (cylinder) is more subtle. In our anlaysis, we consider two types of countings. In case I, s_2 will be between s_0 and $s_0 s/\bar{s}$ as before. In case II, the upper limit is taken as $s_0 s/s_1$. This choice is motivated by the fact that in a cylinder topology, there are at least two clusters in a multiperipheral chain. Therefore, if one of the clusters has energy s_1, the other can have up to $s_0 s/s_1$. We will find later that the case II gives a reasonable output for the Pomeron intercept and slope. The case I leaves out too much of the configuration and hence generates a lower pole. We also find that only in the peak approximation these two countings

give the same results.

The integral equation (for case II) of the Pomeron is (subscript PC stands for planar plus cylinder level),

$$A_{PC}(s,t) = P_0(s,t) + T_{PC}(s,t) \ , \tag{12}$$

where (similar to Eq. (11)),

$$T_{PC}(s,t) = \frac{1}{8\pi^2} \int_{s_0}^{\bar{s}} ds_1 P_0(s_1,t) \left[\int_{s_0}^{s_0 s/\bar{s}} ds_2 z_2 + \int_{s_0}^{s_0 s/s_1} ds_2 \right]$$

$$\iint dt_2 dt_2' \frac{\theta(-\Delta)}{|\Delta|^{1/2}} g^2(t,t_2,t_2') \left(\frac{s}{s_1 s_2}\right)^{\alpha_2 + \alpha_2'} A_{PC}(s_2,t) \tag{13}$$

The only difference in the case I is that the upper limit of s_2 integration is $s_0 s/\bar{s}$ in the second term also.

Our integral equation for Pomeron (see also Refs. 6, 7 and 10) differs from that of the works of Refs. 2, 4, 13 and 14. These authors use the Reggeon bootstrap to replace the sum represented by the cutoff (dotted) propagator by a pure pole. But we shall see later that there will be cuts present in addition to the pure pole s^{α}. It has been shown that for $s < 100$ Gev^2, the cut contribution is 9% or more of the pole term. We, therefore, prefer not to use a pure Regge pole as the inhomogeneous term.[17]

Integrations over t_2 and t_2': In equations (11) and (13) we choose the vertex functions as,[7,13]

$$g^2(t,t_2,t_2') = k^2(\alpha(t) - \alpha_{c_2})^2 \, e^{at+b(t_2+t_2')} \quad , \qquad (14a)$$

$$\text{with } \alpha_{c_2} = \alpha(t_2) + \alpha(t_2') - 1 \qquad (14b)$$

The presence of the factor $(\alpha(t) - \alpha_{c_2})^2$ is due to the planar duality.[11,13] The integration over t_2 and t_2' can now be performed analytically. The result is given in Eq. (A-4). We expand Eq. (A-4) for small values of t by neglecting terms of order (t/s) compared with $\alpha' t$ and $(\alpha' t)^2$. The large negative exponentials appearing in the hyperbolic functions are also neglected. We then get, after using Eqs. (10), (12) and (A-4),

$$A(s,t) = P_0(s,t) + \frac{k^2 e^{at}}{16\pi s} \int_{s_0}^{\bar{s}} ds_1 P_0(s_1,t) \int_{s_0}^{s_0 s/\bar{s}} ds_2 A(s_2,t)$$

$$\left(\frac{s}{s_1 s_2}\right)^{2\alpha_0 + 2\alpha' t_{min}} e^{2bt_{min}} \, e^{p \frac{tr^2}{2}\left(1 - \frac{s_2}{s}\right)}$$

$$\left\{ \frac{(\alpha(t) - 2\alpha_0 + 1 - 2\alpha' t_{min})^2}{\left(b + \alpha' \ell n \frac{s}{s_1 s_2}\right)} + \frac{2\alpha'(\alpha(t) - 2\alpha_0 + 1 - 2\alpha' t_{min})}{\left(b + \alpha' \ell n \frac{s}{s_1 s_2}\right)^2} \right.$$

$$\left. + \frac{2\alpha'}{\left(b + \alpha' \ell n \frac{s}{s_1 s_2}\right)^3} \right.$$

$$+\alpha' t\left(1-\frac{1}{2}r^2\right)\left(1-\frac{s_2}{s}\right)\left[\frac{-\alpha'}{\left(b+\alpha'\ln\frac{s}{s_1s_2}\right)^2}\right.$$

$$\left.-\frac{2(\alpha(t)-2\alpha_0+1-2\alpha' t_{min})}{\left(b+\alpha'\ln\frac{s}{s_1s_2}\right)}\right]$$

$$+\frac{3\alpha'^2 t\left(1-\frac{s_2}{s}\right)\left(\frac{3}{2}r^2-2\right)}{\left(b+\alpha'\ln\frac{s}{s_1s_2}\right)^2}+\frac{\alpha'^2t^2(1-r^2)^2\left(1-\frac{s_2}{s}\right)^2}{\left(b+\alpha'\ln\frac{s}{s_1s_2}\right)}\Bigg\}$$

$$+\epsilon\frac{k_e^2 at}{16\pi s}\int_{s_0}^{\bar{s}}ds_1 P_0(s_1,t)\int_{s_0}^{s_0 s/s_1}ds_2\, A(s_2,t)\,[r\leftrightarrow 1] \qquad (15)$$

Here A stands for $A_P(A_{PC})$ and ϵ is O(1). t_{min} is the minimum value of t_2 and t_2', and is given by,

$$t_{min} = -\frac{1}{2s}(\lambda^* - \sqrt{\lambda\lambda''}) \ , \qquad (16)$$

where λ, λ'' and λ^* are defined in Eq. (A-3). By expanding Eq. (16), we get to leading power of s_1/s and m^2/s (we take $m_a^2 = m_b^2 = m^2$ for simplicity),

$$t_{min} = -\frac{s_1 s_2}{s-s_2}+\frac{s_2 m^2}{s} \ . \qquad (17)$$

In the above we have not made any expansion in s_2/s, because s_2/s is not necessarily small. If s_2/s is small, we will get, $t_{min} = -s_1s_2/s$ as given in the Introduction.

The corresponding expression of Eq. (15) for the case $t_{min} = 0$ is given in Appendix B (Eq. B-1).

Asymptotic solutions of the integral equations: From the integral equations for Reggeon and Pomeron [Eq. (15)] we will now show that asymptotically in both cases, a pole type solution exists. For the Reggeon case if we put $A_p(s_2,t) = s_2^{\alpha(t)}$ on the right-hand side of Eq. (15), and define a variable $z = s_2/s$, then we get,

$$A_p(s,t) = P_0(s,t) + s^{\alpha(t)} \int_{s_0}^{\bar{s}} ds_1 P_0(s_1,t) s_1^{-2\alpha_0}$$

$$\int_{s_0/s}^{s_0/\bar{s}} dz\, z^{\alpha(t)-2\alpha_0} L(s_1,z,a,b,k,t,r) \ , \qquad (18)$$

where L is defined in Eq. (A-6). It can be seen that asymptotically when $s_0/s \to 0$, then Eq. (18) becomes,

$$A_p(s,t) \xrightarrow[s\to\infty]{} P_0(s,t) + (\text{const})\cdot s^{\alpha(t)} \ . \qquad (19)$$

$P_0(s,t)$ is chosen to be the absorptive part of the amplitude for $s_0 < s < \bar{s}$ and has the form,

$$P_0(s,t) = \theta(s-s_0)\theta(\bar{s}-s)s^{\alpha(t)} \ . \qquad (20)$$

Therefore, asymptotically the solution to $A_p(s,t)$ is a pole

provided the coefficient of $s^{\alpha(t)}$ on the right-hand side of Eq. (19) is 1, i.e.,

$$1 = \int_{s_0}^{\bar{s}} ds_1 P_0(s_1,t) s_1^{-2\alpha_0} \int_0^{s_0/\bar{s}} dz\ z^{\alpha(t)-2\alpha_0}\ L(s_1,z,a,b,k,t,r)\ . \tag{21}$$

Eq. (21) will be referred to as the planar bootstrap equation.

For the Pomeron case, we can put $A_{PC}(s,t) = s^{\alpha_P(t)}$ in the right-hand side of Eq. (15) and obtain in a similar way,

$$A_{PC}(s,t) = P_0(s,t) + s^{\alpha_P(t)} \int_{s_0}^{\bar{s}} ds_1 P_0(s_1,t) s_1^{-2\alpha_0} \left[\int_{s_0/s}^{s_0/\bar{s}} dz\ z^{\alpha_P(t)-2\alpha_0}\ L(s_1,z,a,b,k,t,r) + \int_{s_0/s}^{s_0/s_1} dz\ z^{\alpha_P(t)-2\alpha_0}\ L(s_1,z,a,b,k,t,1) \right] \tag{22}$$

As $s \to \infty$, the lower limit of z-integration tends to zero, and the condition for the output Pomeron behaviour is,

$$1 = U + C\ , \tag{23a}$$

where U and C are the contributions from the uncrossed and the crossed kernels. U is given by,

$$U = \int_{s_0}^{\bar{s}} ds_1 P_0(s_1,t) s_1^{-2\alpha_0} \int_0^{s_0/\bar{s}} dz\ z^{\alpha_p(t)-2\alpha_0}\ L(s_1,z,a,b,k,t,r)\ , \tag{23b}$$

and C is obtained by taking r = 1 in the above expression, and taking the upper limit of z integration to be s_0/s_1.

The Cut Contributions: There will, however, be cuts present in the output amplitude $A_p(s,t)$. The terms of the following form in Eq. (15),

$$\frac{\left(\frac{s}{s_1 s_2}\right)^{2\alpha_0+2\alpha' t_{min}}}{[b + \alpha' \ln \frac{s}{s_1 s_2}]^n}\ ,$$

(where n is the appropriate integer power of different terms) are the characteristic of the Reggeon-Reggeon cuts. The total cut contribution can be found by using the lower limit of the z integration in Eq. (18). We call this term which has the total cut as $A_{p,cut}(s,t)$. This is given by

$$A_{p,cut}(s,t) = -s^{\alpha(t)} \int_{s_0}^{\bar{s}} ds_1 P_0(s_1,t) s_1^{-2\alpha_0} \int_0^{s_0/s} dz\ z^{\alpha(t)-2\alpha_0}$$

$$L(s_1,z,a,b,k,t,r)\ . \tag{24}$$

By using Eq. (A-6) in Eq. (24), it can be seen that the

leading cut contribution at $t = 0$ is of order $s^{2\alpha_0 - 1}$ (within factors of lns). We call this term $\bar{A}_{P,cut}(s,0)$ which is given by,

$$\bar{A}_{P,cut}(s,0) = -\frac{k^2}{16\pi} s^{\alpha_0} \int_{s_0}^{\bar{s}} ds_1 P_0(s_1,0) s_1^{-2\alpha_0} \int_0^{s_0/s} dz\, z^{-\alpha_0}$$

$$(s_1 z)^{2\alpha' z\left(\frac{s_1}{1-z} - m^2\right)} e^{-2bz\left(\frac{s_1}{1-z} - m^2\right)}$$

$$\left\{ \frac{(1-\alpha_0)^2}{b - \alpha' \ln s_1 z} + \frac{2\alpha'(1-\alpha_0)}{(b - \alpha' \ln s_1 z)^2} + \frac{2\alpha'^2}{(b - \alpha' \ln s_1 z)^3} \right\}. \quad (25)$$

The Pomeron, like the planar case, contains cut contributions also. The leading cut contribution is, as before, of order $s^{2\alpha_0 - 1}$ (within factors of lns). This part, $\bar{A}_{PC,cut}(s,0)$ [at $t = 0$] is given by [here $\alpha_p^0 = \alpha_p(0)$],

$$\bar{A}_{PC,cut}(s,0) = -\frac{k^2}{16\pi} s^{\alpha_p^0} \int_{s_0}^{\bar{s}} ds_1 P_0(s_1,0) s_1^{-2\alpha_0}$$

$$\left[\int_0^{s_0/\bar{s}} dz + \int_0^{s_0/s_1} dz \right] z^{\alpha_p^0 - 2\alpha_0}$$

$$(s_1 z)^{2\alpha' z\left(\frac{s_1}{1-z} - m^2\right)} e^{-2bz\left(\frac{s_1}{1-z} - m^2\right)}$$

$$\left\{ \frac{(1-\alpha_0)^2}{(b - \alpha' \ln s_1 z)} + \frac{2\alpha'(1-\alpha_0)}{(b - \alpha' \ln s_1 z)} + \frac{2\alpha'^2}{(b - \alpha' \ln s_1 z)^3} \right\}. \quad (26)$$

For $t_{min} = 0$, the equations derived here have to be modified. In Appendix B, we give the modified versions of Eqs. (25) and (26).

IV. NUMERICAL RESULTS AND COMPARISONS

In this section, we present the results of the numerical calculations.

i) Pomeron intercept, slope and the triple-Regge vertex: For the purpose of calculation, we fix the parameters $\bar{s}$ = 5 GeV^2, α_0 = .5, α' = 1 GeV^{-2} and $m^2 = s_0$ = 1 GeV^2. The planar bootstrap equation (21) still has three parameters, a, b and k. At t = 0, only b and k appear. For each value of b, we have solved for k. We then solve Eq. (23a) for the intercept of the Pomeron α_p^0 using these values of b and k. For small but nonzero t, we can eliminate the parameter a between the above equations and obtain $\alpha_p(t)$. For small values of t, one can make a linear expansion for $\alpha_p(t) = \alpha_p^0 + \alpha_p' t$, and from there calculate α_p'. We therefore establish a relation between b, k, α_p^0 and α_p'.

The nominal ranges of α_p^0 and α_p' lie between .85 and .97,[18] and .1 and .5,[20] respectively. The value of k has been estimated[23] to be 9.8 (in GeV units) within an uncertainty of about 25%. In Fig. 5a we have plotted α_p^0 and α_p' as a function of b. For a direct comparison between α_p^0 and α_p', we show them in Fig. 5b. It may be seen that when we compare our numbers with the above-quoted numbers, we find that our model becomes very restrictive. We consider the reasonable ranges of α_p^0 and α_p' and find the limits on b and k. This gives,

$$.94 > \alpha_p^0 > .85 \qquad .1 < \alpha_p' < .5$$
$$1.5 < b < 2.0 \qquad 12.1 < k < 15.2 \tag{27}$$

A typical solution is, for example, $b = 1.6$, $\alpha_p^0 = .92$, $\alpha_p' = .2$ and $k = 12.9$.

Note that b is very restrictive within a small range. We shall compare below our triple Regge parametrization with those obtained by phenomenological fits to the data. The value of k is obtained by performing the planar bootstrap. We have also checked that this is consistent with the loop expansion (up to three loops) of the amplitude (see below). As stated in the footnote 23, the estimate of k by Chan et al. is based on a calculation up to two loops. We find that our value of k is comparable to the empirical estimate obtained by them.

We have found[24] that the solution for Pomeron satisfies the asymptotic planarity property at positive values of t. For $b = 1.6$, spin 2 particles give,

$$M_{A_2}^2 - M_f^2 = .03 \text{ GeV}^2 ,$$

while the experimental value is $.1 \text{ GeV}^2$. The result should improve when the baryon exchange is taken into account. Our results are very similar to the previous works on this.[7,13,19]

We shall now compare the t-dependence of our triple-Regge vertex with other parametrizations in the literature.[3,21,22] The main difficulty in comparing different works is that while Ref. 3 (and also the present work) has only one basic vertex, in other works (e.g. Refs. 21 and 22) there are vertices corresponding to triple Pomeron, Pomeron-Pomeron-Reggeon, Reggeon-Reggeon-Pomeron and triple-Reggeon. Due to nonleading nature of the triple-Regge vertex, there is large uncertainty in determining its t-dependence (for more discussions, see Ref. 7). In Fig. 5c we have plotted our vertices $g(0,t_1,t_1)$ for b = 1.5 and 2 (lines a and b) together with those of other references. It is found that none of these vertices lie within our limits a and b. We feel that an analysis of the data with a single vertex is needed in order to make a better comparison with our model.

We have also investigated the possibility when the counting prescription of both uncrossed and the crossed diagrams are the same (counting I, i.e., in Eq. (15), we use the upper limit of s_2 to be $s_0 s/\bar{s}$ also). The result of this calculation is shown in Fig. 6a and 6b. It can be seen that the intercept α_P^0 is substantially lower here. For α_P' between .5 and 0, α_P^0 lies between .75 and .80. Note that k is the same as the previous case, because the planar equation is unchanged. The reason for the lower intercept here

is the fact that a substantial amount of phase space is left out in this counting. It is interesting to note that Ref. 9, which uses counting I, gets a Pomeron intercept of .75 (their Reggeon intercept is .57). Although these authors neglect t_{min}, we will see later that this effect is not very important for counting I.

The relative importance of the planar and cylinder terms in the Pomeron equation [see Eq. (23b)] is studied by calculating the ratio $R \equiv C/U$. For counting I, this ratio is 1. In Fig. 7, the ratio R (for counting II) is plotted as a function of b. It is seen that for small values of b, the ratio is significantly different from 1. At higher values of b, this ratio approaches one. The reason is that the upper limit of z integration in Eq. (23b) contributes negligibly due to t_{min} effect. We see that for $t_{min} = 0$, the ratio is substantially higher at all b.

Since many works in the literature are done by putting $t_{min} = 0$, we want to compare our work with theirs by taking $t_{min} = 0$. In the last paragraph, we have already discussed the effect of t_{min} on the cylinder to planar coupling ratios R. Here we will discuss its effect on the Pomeron intercept. In Fig. 5a and 6a the broken lines give the Pomeron intercept at $t = 0$. We find that in both cases, this effect raises the value of the Pomeron intercept. However, this effect is more important in the case of counting II. This is because

here s_2 can have higher masses, and the average value of t_{min} is higher. It is interesting to note that the Pomeron intercept of several previous works which also neglect t_{min} has higher values. In our case, taking b = 1.6, we find the following:

Counting I: $\alpha_p^0 = .78$

Counting II: $\alpha_p^0 = 1.27$

Refs. 5, 7 and 13 have Pomeron intercepts as 1.62, 1.27 and 1.1, respectively. However, the amount increased is sensitive to the counting procedure. Ref. 5 has used counting II. Refs. 7 and 13 have done double counting both at the planar and the cylinder levels. They have used s as the upper limit of s_2 integration for both planar and cylinder diagrams.

ii) Cuts and lower singularities: We will now examine the behaviour of the amplitudes (both the Reggeon and the Pomeron) at nonasymptotic energies. It is seen that due to the presence of cuts and other lower singularities, the amplitude deviates from the pure pole behaviour at low energy. We will take t = 0 and b = 1.6 for the calculation.

Reggeon: From Eq. (18), we calculate $A_p(s,0)/s^{\alpha_0}$ and plot it as a function of s. (Note that for $s > \bar{s}$, the inhomogeneous term $P_0(s,0) = 0$.) This is shown as line A in Fig. 8. If no cut or other singularity is present, then this line would have a constant value of 1 (shown as line A'). We also calculate the leading cut contribution given

by Eq. (25). The line A" is given by $1 + \bar{A}_{p,cut}(s,0)/s^{\alpha_0}$, and this, of course, approaches 1 as $s \to \infty$. It can be seen that cut contribution is negligible at higher energies. For example, at 100 GeV^2, the cut contribution is only 9% of the pole. The difference between the lines A' and A" represents the contribution due to lower lying singularities (smaller than $s^{2\alpha_0-1}$).

One can do a similar analysis for $t_{min} = 0$ and compare it with the previous case. The modified formulas for this case are given in the Appendix B. The line B in Fig. 8 is $A_p(s,0)/s^{\alpha_0}$, and B' is the asymptotic value of this line. The cut contribution is just the difference between B and B'. Note that unlike the previous case, here the cut contribution is of order $s^{2\alpha_0-1}$ [see Eq. (B-4)].

Pomeron: For the Pomeron case, we plot similar graphs like the planar case by using Eqs. (22), (23a) and (26). These are lines A, A' and A" of Fig. 9. Similar plots are also given for the case $t_{min} = 0$ by using the modified formulas given in Appendix B. Once again, it can be seen that the contribution of cuts and other lower singularities are small at moderate energies.

We have shown here that both for the Reggeon and the Pomeron cases the contribution of cut is quantitatively negligible. Previously we reached the same conclusions[7] using the J-plane analysis.

iii) Iterative solutions: Here we make an iterative approach to solve Eq. (15) for both the Reggeon and the Pomeron amplitudes at t = 0. This method shows how clusters contribute to the imaginary part of the total amplitude at some energy. This also gives the normalization (or residue) of the amplitudes which cannot be obtained from the asymptotic solutions discussed previously. We then compare these residues with those obtained from Eqs. (C-4) and (C-6) and verify that to high accuracy they are approximately the same. The ratio of Pomeron to Reggeon couplings are also found.

For the Reggeon amplitude, we get, after iterating on the right-hand side of Eq. (15),

$$A_p(s,0) = P_0(s,0) + I_{1,p}(s,0) + I_{2,p}(s,0) + \cdots . \quad (28)$$

$I_{n,p}(s,0)$ is the contribution of a diagram with n uncrossed loops. We have calculated $I_{n,p}$'s for several n and for s up to 600 GeV^2. The value of k (= 12.9 for b = 1.6) obtained from the bootstrap equation (21) is used. In Fig. 10 we have shown the contribution of the different loops. At higher energies, the sum of the diagrams reaches a behaviour $c_p s^{\alpha_0}$. The constant c_p is found from the figure to be .55.

We can do the same iterative method for the Pomeron amplitude. In the same way, we get,

$$A_{PC}(s,0) = P_0(s,0) + I_{1,PC}(s,0) + I_{2,PC}(s,0) + \cdots . \quad (29)$$

Here $I_{n,PC}$ is the sum of all diagrams with n loops (both crossed and uncrossed). Due to large contributions of the cylinder diagrams (because of counting) the sum of the loops already approaches the asymptotic behaviour $c_{PC}s^{\alpha_P^0}$ for relatively small s. We have calculated the loops up to $s = 250\ GeV^2$. The value of c_{PC} is found to be .50 (see Fig. 11).

c_P and c_{PC} are also found from Eqs. (C-4) and (C-6), and they agree with the residues found in the above method. At t = 0, the ratio of Pomeron to Reggeon residue $c \equiv c_{PC}/c_P$ is found to be .91 which is in reasonable agreement with the empirical value[4] which lies between .9 and 1.2.

Chan[3,4] et al. have also performed a similar calculation using the loop expansion. But they have used a different integral equation (see section III) and also different NDC. Their ratio of Pomeron to Reggeon coupling is 1.0.

V. SUMMARY

We have studied the DTU program at the planar and the cylinder levels by incorporating the NDC condition and t_{min} effect. For simplicity, SU(N) symmetry is assumed to be exact.

The relation between the NDC condition and the production mechanism of the multiparticles is investigated. The average separation between two clusters is calculated using the models of Chan et al.[3,4] and Finkelstein and Koplik.[9] This may serve as a test to determine which NDC is preferable. We find that the prescription of Refs. 4 and 9 give a cluster separation of approximately 1/a and 2/a respectively (where 1/a is average interparticle spacing). In studying our Reggeon and Pomeron equations, we have used the prescription of Ref. 9 since the Regge behaviour of the amplitude is better if the clusters are more widely separated.

The Reggeon (planar) integral equation is set up and the bootstrap condition is derived. For the Pomeron integral equation, one needs both the planar and the cylinder diagrams. Two countings are studied for the cylinder diagrams and one of them (counting II) is favoured. Our model finds a relation between the Pomeron parameters α_p^0 and α_p' (at $t = 0$) and the triple-Regge parameters k and b. Our model puts the following restrictions on these physical quantities: $.94 > \alpha_p^0 > .85$, $.1 < \alpha_p' < .5$, $1.5 < b < 2.0$ and

and $12.1 < k < 15.2$. A typical solution in the above range is $\alpha_P^0 = .92$, $\alpha_P' = .2$, $k = 12.9$ and $b = 1.6$.

The effect of neglecting t_{min} is also studied and it is found that the neglect of t_{min} gives rise to substantially higher Pomeron intercept. The difference is about .2 to .3 units for counting II (for counting I, it is about .1).

The Reggeon and the Pomeron equations are also studied at nonasymptotic energies. It is found that although cuts and other lower singularities are present in both cases, their contributions are small compared to the corresponding poles at moderate energies ($s > 100$ GeV^2).

The Reggeon and the Pomeron equations are further investigated by using a loop expansion. We find that the sum of the loops reaches a constant in each case. As expected, these constants turn out to be the same as obtained from the J-plane analysis. We also find that the ratio of Pomeron to Reggeon residues is equal to .91.

We find that in the peak approximation ($b \to \infty$), the Pomeron intercept does not tend to 1 (see Figs. 5a and 6a), which is the famous result of Lee and Veneziano.[25] It was shown[7] that Lee-Veneziano relation is valid if t_{min} is neglected, and no double counting conditions are not imposed. Both t_{min} and NDC introduce correlations[14] among the clusters, and the Lee-Veneziano relation is not valid. All that can be said is that $\alpha_P^0 > \alpha_0$.[26] At higher positive values of t,

$\alpha_p(t)$ approaches $\alpha(t)$, and thus satisfies precocious asymptotic planarity.

Acknowledgements

I am grateful to Professor Charles B. Chiu for his guidance and constructive criticisms during the progress of this work. I also thank Dr. Don M. Tow for reading the manuscript and for his comments. This work was supported in part by the U.S. Department of Energy under Contract No. EY-76-S-05-3992.

APPENDIX A

The phase space integration is given by (see also Ref. 3),

$$\int_{P.S.} = \int ds_1 \int ds_2 \int \frac{d^4k_1}{(2\pi)^3}\,\delta^+(k_1^2 - s_1) \int \frac{d^4k_2}{(2\pi)^3}\,\delta^+(k_2^2 - s_2)$$

$$(2\pi)^4\delta^4(k_1 + k_2 - P)$$

$$= \frac{1}{8\pi^2} \int ds_1 \int ds_2 \int dt_2 \int dt_2' \, \frac{\theta(-\Delta)}{|\Delta|^{1/2}} \qquad \text{(A-1)}$$

The limits of t_2 and t_2' integrations are determined by the θ-function, and the function Δ is defined as,

$$\Delta = \lambda(t_2^2 + t_2'^2) - 2t_2t_2'(\lambda + 2st) - 2t\lambda^*(t_2 + t_2') + t^2\lambda''$$

$$+ \frac{t}{s}(\lambda''\lambda - \lambda^{*2}) \,, \qquad \text{(A-2)}$$

where,

$$\lambda = s^2 + m_a^4 + m_b^4 - 2sm_a^2 - 2sm_b^2 - 2m_a^2m_b^2$$

$$\lambda'' = s^2 + s_1^2 + s_2^2 - 2ss_1 - 2ss_2 - 2s_1s_2$$

$$\lambda^* = s^2 + m_a^2s_1 + m_b^2s_2 - ss_1 - ss_2 - m_a^2s - m_a^2s_2 - m_b^2s - m_b^2s_1 \,. \qquad \text{(A-3)}$$

Integrations over t_2 and t_2' in Eqs. (11) and (13) are tedious, but straightforward. The integrations are performed by using the method of Ref. 3 (see their Eq. (40)). For the Reggeon (Pomeron) case, we take,

$$T(s,t) = T_P(s,t)[T_{PC}(s,t)] \ ,$$

$$A(s_2,t) = A_P(s_2,t)[A_{PC}(s_2,t)] \ ,$$

and, $\varepsilon = 0$ (1). The result is,

$$T(s,t) = \frac{k_0^2 at}{8\pi s} \int_{s_0}^{s} ds_1 P_0(s_1,t) \int_{s_0}^{s_0 s/s_1} ds_2 A \quad (s_2,t) \left(\frac{s}{s_1 s_2}\right)^{2\alpha_0}$$

$$\sqrt{\frac{\lambda''}{B}} \exp\left(-\frac{p}{s}\lambda^*\right) \Bigg\{ (\alpha(t) - 2\alpha_0 + 1)^2 \sinh\sqrt{B}$$

$$- 2\alpha'(\alpha(t)-2\alpha_0+1) \Bigg[-\frac{\lambda^*}{s} \sinh\sqrt{B}$$

$$+ \frac{\lambda\lambda''}{s^2}\left(1+\frac{st}{\lambda}\right)p\left(\frac{\cosh\sqrt{B}}{\sqrt{B}} - \frac{\sinh\sqrt{B}}{B}\right)\Bigg]$$

$$+ \alpha'^2\left[\left(\frac{\lambda^*}{s}\right)^2 \sinh\sqrt{B} + \frac{\lambda\lambda''}{s^2}\left(1+\frac{st}{\lambda}\right)\left(1-\frac{\lambda^* p}{s}\right)\left(\frac{\cosh\sqrt{B}}{\sqrt{B}} - \frac{\sinh\sqrt{B}}{B}\right)\right]$$

$$+ \alpha'^2 \frac{\lambda\lambda'' p}{s^2}\left(1+\frac{st}{\lambda}\right)\frac{\lambda^*}{s}\left(\frac{\sinh\sqrt{B}}{B} - \frac{\cosh\sqrt{B}}{\sqrt{B}}\right)$$

$$+ \alpha'^2\left[\frac{\lambda\lambda'' p}{s^2}\left(1+\frac{st}{\lambda}\right)\right]^2\left[\frac{-3\cosh\sqrt{B}}{B^{3/2}} + \frac{\sinh\sqrt{B}}{B} + \frac{3\sinh\sqrt{B}}{B^2}\right]\Bigg\}$$

$$+\epsilon\,\frac{k^2 e^{at}}{8\pi s}\int_{s_0}^{\bar{s}} ds_1 P_0(s_1,t)\int_{s_0}^{s_0 s/s_1} ds_2 \Lambda\ (s_2,t)\left(\frac{s}{s_1 s_2}\right)^{2\alpha_0}\sqrt{\frac{\lambda''}{B'}}$$

$$\exp\left(-\frac{p}{s}\lambda^*\right)\Bigg\{\left(\alpha(t)-2\alpha_0+1\right)^2\sinh\sqrt{B'} - 2\alpha'\left(\alpha(t)-2\alpha_0+1\right)$$

$$\left[-\frac{\lambda^*}{s}\sinh\sqrt{B'} + \frac{\lambda\lambda''}{s^2}\left(1+\frac{st}{\lambda}\right)p\left(\frac{\cosh\sqrt{B'}}{\sqrt{B'}} - \frac{\sinh\sqrt{B'}}{B'}\right)\right]$$

$$+\alpha'^2\left[\left(\frac{\lambda^*}{s}\right)^2\sinh\sqrt{B'}\right.$$

$$\left.+\frac{\lambda\lambda''}{s^2}\left(1+\frac{st}{\lambda}\right)\left(1-\frac{\lambda^* p}{s}\right)\left(\frac{\cosh\sqrt{B'}}{\sqrt{B'}} - \frac{\sinh\sqrt{B'}}{B'}\right)\right]$$

$$+\alpha'^2\,\frac{\lambda\lambda'' p}{s^2}\left(1+\frac{st}{\lambda}\right)\frac{\lambda^*}{s}\left(\frac{\sinh\sqrt{B'}}{B'} - \frac{\cosh\sqrt{B'}}{\sqrt{B'}}\right)$$

$$+\alpha'^2\left[\frac{\lambda\lambda'' p}{s^2}\left(1+\frac{st}{\lambda}\right)\right]^2\left[\frac{-3\cosh\sqrt{B'}}{B'^{3/2}} + \frac{\sinh\sqrt{B'}}{B'} + \frac{3\sinh\sqrt{B'}}{B'^2}\right]\Bigg\} \qquad \text{(A-4)}$$

In the above expression,

$$p = b + \alpha' \ell n \frac{s}{s_1 s_2}$$

$$r^2 = 1 + \pi^2\alpha'^2/p^2$$

$$B = \frac{\lambda\lambda'' p^2}{s^2}\left(1 + \frac{str^2}{\lambda}\right) \qquad \text{(A-5)}$$

$$B' = \frac{\lambda\lambda'' p^2}{s^2}\left(1 + \frac{st}{\lambda}\right)$$

$$\alpha(t) = \alpha_0 + \alpha' t$$

We have verified that when t_{min} and NDC conditions are neglected, Eq. (A-4) reproduces the corresponding equations of Ref. 7. The function $L(s_1,z,a,b,k,t,r)$ in Eq. (18) of the text is defined as,

$$L(s_1,z,a,b,k,t,r) = \frac{k^2 e^{at}}{16\pi} (s_1 z)^{2\alpha' z\left(\frac{s_1}{1-z}-m^2\right)} e^{-2bz\left(\frac{s_1}{1-z}-m^2\right)}$$

$$e^{pr^2\frac{2t}{2}(1-z)}\left\{ \frac{\left[\alpha(t)-2\alpha_0+1-2\alpha' z\left(\frac{s_1}{1-z}-m^2\right)\right]^2}{(b-\alpha' \ln s_1 z)} \right.$$

$$+ \frac{2\alpha'\left[\alpha(t)-2\alpha_0+1+2\alpha' z\left(\frac{s_1}{1-z}-m^2\right)\right]}{(b-\alpha' \ln s_1 z)^2} + \frac{2\alpha'^2}{(b-\alpha' \ln s_1 z)^3}$$

$$+ \alpha' t\left(1-\frac{1}{2}r^2\right)(1-z)\left[\frac{\alpha'}{(b-\alpha' \ln s_1 z)^2}\right.$$

$$\left. - \frac{2\left[\alpha(t)-2\alpha_0+1+2\alpha' z\left(\frac{s_1}{1-z}-m^2\right)\right]}{(b-\alpha' \ln s_1 z)}\right]$$

$$\left. + \frac{3\alpha'^2 t(1-z)\left(\frac{3}{2}r^2-2\right)}{(b-\alpha' \ln s_1 z)^2} + \frac{\alpha'^2 t^2 (1-r^2)^2 (1-z)^2}{(b-\alpha' \ln s_1 z)} \right\} . \qquad \text{(A-6)}$$

The modification of Eq. (A-6) for $t_{min} = 0$ is given in Eq. (B-4).

APPENDIX B

Modifications of Eqs. (15), (25), (26) and (A-6) for $t_{min} = 0$: Eq. (15) becomes,

$$A(s,t) = P_0(s,t) + \frac{k^2 e^{at}}{16\pi s} \int_{s_0}^{\bar{s}} ds_1 P_0(s_1,t) \int_{s_0}^{s_0 s/\bar{s}} ds_2 \; A(s_2,t)$$

$$\left(\frac{s}{s_1 s_2}\right)^{2\alpha_0} e^{p\frac{tr^2}{2}\left(1-\frac{s_2}{s}\right)} \left\{ \frac{(\alpha(t)-2\alpha_0+1)^2}{\left(b+\alpha' \ln \frac{s}{s_1 s_2}\right)} + \frac{2\alpha'(\alpha(t)-2\alpha_0+1)}{\left(b+\alpha' \ln \frac{s}{s_1 s_2}\right)^2} \right.$$

$$\left. + \frac{2\alpha'}{\left(b+\alpha' \ln \frac{s}{s_1 s_2}\right)^3} \right.$$

$$+ \alpha' t \left(1-\frac{1}{2}r^2\right)\left(1-\frac{s_2}{s}\right) \left[\frac{\alpha'}{\left(b+\alpha' \ln \frac{s}{s_1 s_2}\right)^2} - \frac{2(\alpha(t)-2\alpha_0+1)}{\left(b+\alpha' \ln \frac{s}{s_1 s_2}\right)} \right]$$

$$\left. + \frac{3\alpha'^2 t\left(1-\frac{s_2}{s} \quad \frac{3}{2}r^2-2\right)}{\left(b+\alpha' \ln \frac{s}{s_1 s_2}\right)^2} + \frac{\alpha'^2 t^2 (1-r^2)^2 \left(1-\frac{s_2}{s}\right)^2}{\left(b+\alpha' \ln \frac{s}{s_1 s_2}\right)^2} \right\}$$

$$+\varepsilon \frac{k^2 e^{at}}{16\pi s} \int_{s_0}^{\bar{s}} ds_1 P_0(s_1,t) \int_{s_0}^{s_0 s/s_1} ds_2 A \quad (s_2,t)\{r \leftrightarrow 1\} \qquad \text{(B-1)}$$

Eq. (25) becomes,

$$\bar{A}_{P,cut}(s,0) = -\frac{k^2}{16\pi} s^{\alpha_0} \int_{s_0}^{\bar{s}} ds_1 P_0(s_1,0) s_1^{-2\alpha_0} \int_0^{s_0/s} dz\, z^{-\alpha_0}$$

$$\left\{ \frac{(1-\alpha_0)^2}{b-\alpha' \ln s_1 z} + \frac{2\alpha'(1-\alpha_0)}{(b-\alpha' \ln s_1 z)^2} + \frac{2\alpha'^2}{(b-\alpha' \ln s_1 z)^3} \right\} . \quad \text{(B-2)}$$

Eq. (26) becomes,

$$\bar{A}_{PC,cut}(s,0) = -\frac{k^2}{16\pi} s^{\alpha_p^0} \int_{s_0}^{\bar{s}} ds_1 P_0(s_1,0) s_1^{-2\alpha_0} \left[\int_0^{s_0/\bar{s}} dz + \int_0^{s_0/s_1} dz \right] z^{\alpha_p^0 - 2\alpha_0}$$

$$\left\{ \frac{(1-\alpha_0)^2}{b-\alpha' \ln s_1 z} + \frac{2\alpha'(1-\alpha_0)}{(b-\alpha' \ln s_1 z)^2} + \frac{2\alpha'^2}{(b-\alpha' \ln s_1 z)^3} \right\} . \quad \text{(B-3)}$$

Eq. (A-6) of Appendix A changes to,

$$L(s_1,z,a,b,k,t,r) = \frac{k^2 e^{at}}{16\pi} e^{pr^2 \frac{t}{2}(1-z)}$$

$$\left\{ \frac{[\alpha(t)-2\alpha_0+1]^2}{(b-\alpha' \ln s_1 z)} + \frac{2\alpha'[\alpha(t)-2\alpha_0+1]}{(b-\alpha' \ln s_1 z)^2} + \frac{2\alpha'^2}{(b-\alpha' \ln s_1 z)^3} \right.$$

$$+ \alpha' t \left(1 - \frac{1}{2} r^2\right)(1-z) \left[\frac{\alpha'}{(b-\alpha' \ln s_1 z)^2} - \frac{2[\alpha(t)-2\alpha_0+1]}{(b-\alpha' \ln s_1 z)} \right]$$

$$\left. + \frac{3\alpha'^2(1-z)\left(\frac{3}{2}r^2-2\right)}{(b-\alpha' \ln s_1 z)^2} + \frac{\alpha'^2 t^2 (1-r^2)^2 (1-z)^2}{(b-\alpha' \ln s_1 z)} \right\} . \quad \text{(B-4)}$$

APPENDIX C

Here we will solve the Reggeon and the Pomeron integral equations (15) in the J-plane. We also derive the conditions for the output poles and their residues.

The Mellin transform of an amplitude F(s,t) is defined by,

$$F(J,t) = \int_{s_0}^{\infty} s^{-J-1} F(s,t)ds \qquad \text{(C-1)}$$

Using this definition, and after some algebra, we get,

$$A(J,t) = P_0(J,t)\left\{1 - \int_{s_0}^{\bar{s}} ds_1 P_0(s_1,t) s_1^{-2\alpha_0}\left[\int_0^{s_0/\bar{s}} dz\, z^{J-2\alpha_0}\right.\right.$$

$$\left.\left. L(s_1,z,a,b,k,t,r) + \varepsilon\int_0^{s_0/s_1} dz\, z^{J-2\alpha_0} L(s_1,z,a,b,k,t,1)\right]\right\}^{-1}. \qquad \text{(C-2)}$$

In the above expression A stands for A_P (A_{PC}), ε is 0 (1), L is defined in Eq. (A-6), and $P_0(J,t)$ is given by,

$$P_0(J,t) = \frac{\bar{s}^{\alpha(t)-J} - s_0^{\alpha(t)-J}}{\alpha(t) - J}. \qquad \text{(C-3)}$$

Note that $P_0(J,t)$ does not have any singularity at $J = \alpha(t)$. The planar bootstrap equation (21) and the output Pomeron condition (23a) is obtained by requiring that the quantity in

the curly bracket be zero at $J = \alpha(t)$ [or $\alpha_p(t)$ for the Pomeron].

The residue of the Reggeon amplitude $A_p(J,t)$ at $J = \alpha(t)$ is given by,

$$c_p = -\ell n(\bar{s}/s_0)\left[\int_{s_0}^{\bar{s}} ds_1 P_0(s_p,t) s_1^{-2\alpha_0} \int_0^{s_0/\bar{s}} dz\ \ell nz\ z^{-\alpha_0}\ L(s_1,z,a,b,k,t,r)\right]^{-1} . \qquad \text{(C-4)}$$

The amplitude behaves as

$$A_p(J,t) = \frac{c_p}{J - \alpha(t)} , \qquad \text{(C-5)}$$

near $J = \alpha(t)$.

The residue of the Pomeron amplitude at $J = \alpha_p(t)$ is given by,

$$c_{PC} = -P_0(\alpha_p,t)\left\{\int_{s_0}^{\bar{s}} ds_1 P_0(s_1,t) s_1^{-2\alpha_0}\left[\int_0^{s_0/\bar{s}} dz\ z^{\alpha_p - 2\alpha_0}\ell nz\ L(s_1,z,a,b,k,t,r) + \int_0^{s_0/s_1} dz\ z^{\alpha_p - 2\alpha_0}\ell nz\ L(s_1,z,a,b,k,t,1)\right]\right\}^{-1} . \qquad \text{(C-6)}$$

Near $J = \alpha_p(t)$, the Pomeron amplitude is,

$$A_{PC}(J,t) = \frac{c_{PC}}{J - \alpha_p(t)} \, . \qquad \text{(C-7)}$$

References and Footnotes

1. For a review, see, for example, Chan Hong Mo and Tsou Sheung Tsun, Lectures given at Ecole Polytechnique, Paris (1976).
2. G. F. Chew and C. Rosenzweig, Phys. Rev. D12, 3907 (1975); Phys. Lett. 58B, 93 (1975).
3. H. M. Chan et al., Nucl. Phys. B86, 479 (1975).
4. H. M. Chan et al., Nucl. Phys. B92, 13 (1975).
5. J. R. Freeman and Y. Zarmi, Nucl. Phys. B112, 303 (1976).
6. C. B. Chiu, M. Hossain and D. M. Tow, Phys. Rev. D11, 3141 (1976).
7. C. B. Chiu, M. Hossain and D. M. Tow, Phys. Rev. D (to be published).
8. J. R. Freeman, Y. Zarmi, and G. Veneziano, Nucl. Phys. B120, 477 (1977).
9. J. Finkelstein and J. Koplik, Phys. Rev. D14, 1437 (1976).
10. C. Schmid and C. Sorensen, Nucl. Phys. B96, 209 (1975); N. Papadopoulos, C. Schmid, C. Sorensen and D. M. Webber, Nucl. Phys. B101, 189 (1975).
11. C. Rosenzweig and G. Veneziano, Phys. Lett. 52B, 335 (1974); M. M. Schaap and G. Veneziano, Lett. Nuovo Cim. 12, 204 (1975).
12. M. Bishari and G. Veneziano, Phys. Lett. 58B, 445 (1975).
13. M. Bishari, Phys. Lett. 59B, 461 (1975).

14. N. Sakai, Nucl. Phys. B99, 167 (1975).

15. J. Kwiecinski and N. Sakai, Nucl. Phys. B106, 44 (1976).

16. C. Quigg, P. Pirala, and G. H. Thomas, Phys. Rev. D12, 92 (1975).

17. The pure pole behaviour of the Veneziano and Bishari amplitude (Ref. 12 and also Refs. 5 and 8) has been obtained by neglecting the t_{min} effect. This cut cancellation cannot be achieved by using the correct t_{min} factor.

18. Different fits to the experimental data give: $\alpha_p^0 = .85$ [N. Bali and J. Dash, Phys. Rev. D10, 2102 (1974)]; $\alpha_p^0 = .97$ [P. R. Stevens et al., Nucl. Phys. B110, 355 (1976)]; $\alpha_p^0 = .93$ (Refs. 6 and 19). When baryon exchange is considered, the Pomeron is expected to move higher, approximately to 1.04 (Ref. 1).

19. S. T. Tsou, Phys. Lett. 65B, 81 (1976); Preprint SUNY at Stony Brook (1976).

20. For α_p' the different estimates are: .25 (Ref. 4); .4 (Ref. 19); .2 [J. W. Dash, Phys. Lett. 61B, 199 (1976)]; $.3 \pm .2$ (Ref. 1); .5 (Ref. 21); and .36-.37 (Ref. 22).

21. D. P. Roy and R. G. Roberts, Nucl. Phys. B77, 240 (1974).

22. R. D. Field and G. C. Fox, Nucl. Phys. B80, 367 (1974).

23. Our normalization differs from that of Ref. 3. Their g^2 is related to our k^2 as $g^2N = \pi^2k^2/8$. The value of k has been crudely found in Ref. 3. Their k is chosen in such a way that the sum of the first two loops gives

a constant total cross section for K^+p scattering within about 10%. The agreement of their estimate with the $K^-p \to K^0X$ data is within 15%. Therefore k may be uncertain by about 25%.

24. M. Hossain, Ph.D. Thesis, The University of Texas at Austin (1978), unpublished.

25. H. Lee, Phys. Rev. Lett. 30, 719 (1973); G. Veneziano, Phys. Lett. 43B, 413 (1973).

26. G. Veneziano, Nucl. Phys. B74, 365 (1974).

Figure Captions

1. NDC condition of the clusters in the model of Ref. 9. Δ_1 is the average separation between two clusters whose maximum size is L.

2. NDC conditions in the model of Refs. 3 and 4. L_1 and L_2 are the two clusters, and Δ_2 is the average separation between them.

3. Integral equation for the Reggeon amplitude ab → ab.

4. Integral equation for the Pomeron amplitude ab → ab.

5. Pomeron intercept and slope with counting II.
   (a) α_P^0 and α_P' versus b. The dotted line gives α_P^0 for $t_{min} = 0$.
   (b) α_P' versus α_P^0.
   (c) Various parameterizations of the t_1 dependence of the triple Regge vertex: CPT (Ref. 3), RR (Ref. 21) and FF (Ref. 22), our case a and b (see text).

6. Pomeron intercept and slope with counting I.
   (a) α_P^0 and α_P' versus b. The dotted line gives α_P^0 for $t_{min} = 0$.

(b) α_P' versus α_P^0.

7. Ratio R = C/U (Eq. (23b)) versus b for two cases:
(a) $t_{min} \neq 0$; (b) $t_{min} = 0$.

8. $A_P(s,0)/s^{\alpha_0}$ versus s in two cases: (a) $t_{min} \neq 0$;
(b) $t_{min} = 0$.
(a) Line A is $A_P(s,0)/s^{\alpha_0}$ as given in Eq. (18). A' is the line for pure pole behaviour. A" is obtained by including the pole and the next leading term (cut).
(b) Line B is $A_P(s,0)/s^{\alpha_0}$ as given in Eq. (18). B' is the line for pure pole behaviour.
The normalization is chosen so that A' = 1.

9. $A_{PC}(s,0)/s^{\alpha_P^0}$ versus s in two cases: (a) $t_{min} \neq 0$;
(b) $t_{min} = 0$.
(a) Line A is $A_{PC}(s,0)/s^{\alpha_P^0}$ as given in Eq. (22). A' is the line for pure pole behaviour. A" is obtained by including the pole and the next leading term (cut).
(b) Line B is $A_{PC}(s,0)/s^{\alpha_P^0}$ as given in Eq. (22). B' is the line for pure pole behaviour.
The normalization is chosen so that A' = 1.

10. Different loop contributions $I_{n,p}/s^{\alpha_0}$ versus s for the Reggeon case. The broken line is the constant c_p defined in Appendix C.

11. Different loop contributions $I_{n,PC}/s^{\alpha_P^0}$ versus s for the Pomeron case. The constant c_{PC} (defined in Appendix C) is .5.

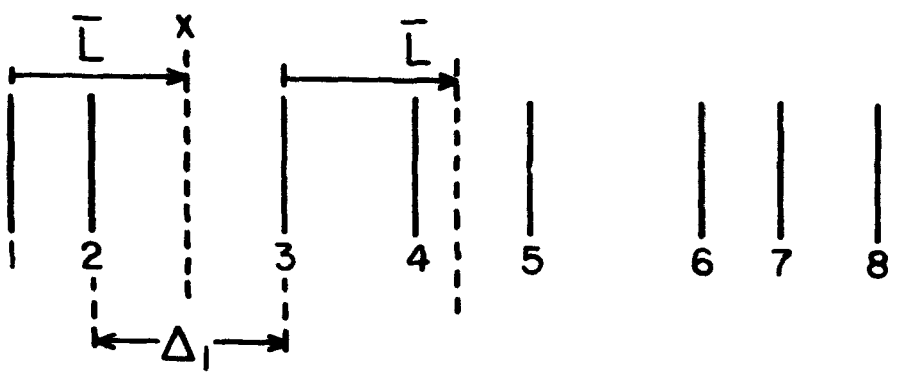

Fig. 1

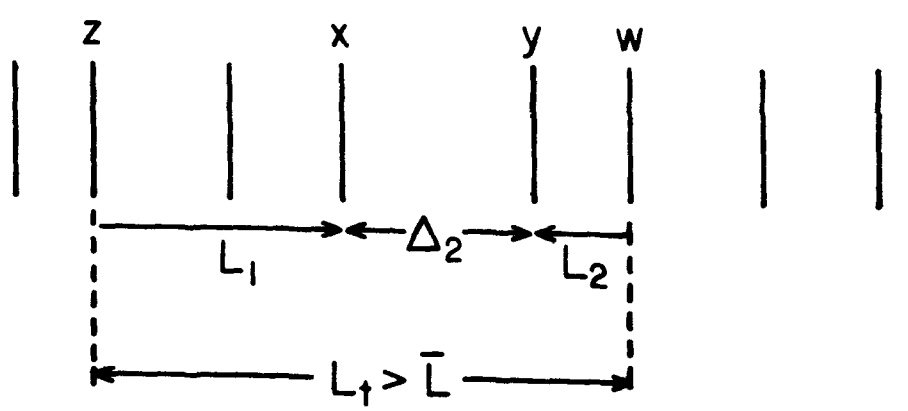

Fig. 2

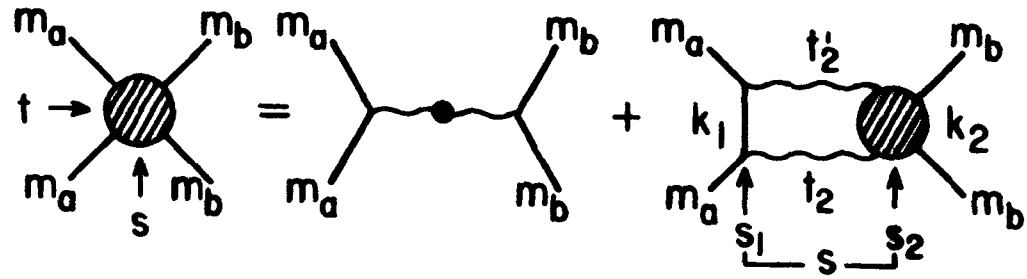
m_a
m_b
t
m_a
m_b
s
=
m_a
m_b
m_a
m_b
+
m_a
t_2'
m_b
k_1
k_2
m_a
t_2
m_b
s_1
s
s_2

Fig. 3

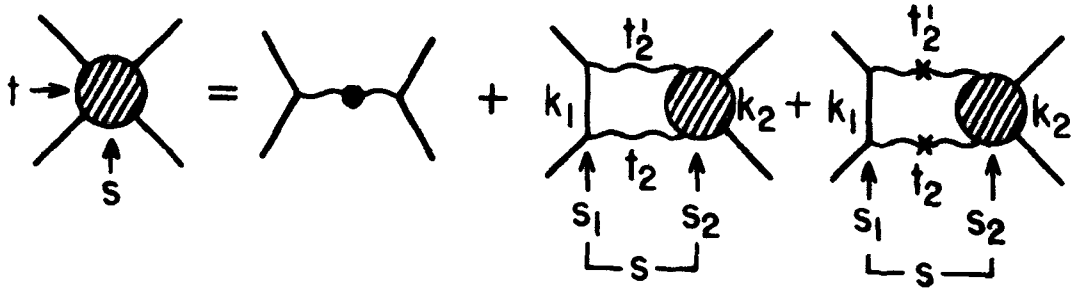
t
s
=
+
t_2'
k_1
k_2
t_2
s_1
s_2
s
+
t_2'
k_1
k_2
t_2
s_1
s_2
s

Fig. 4

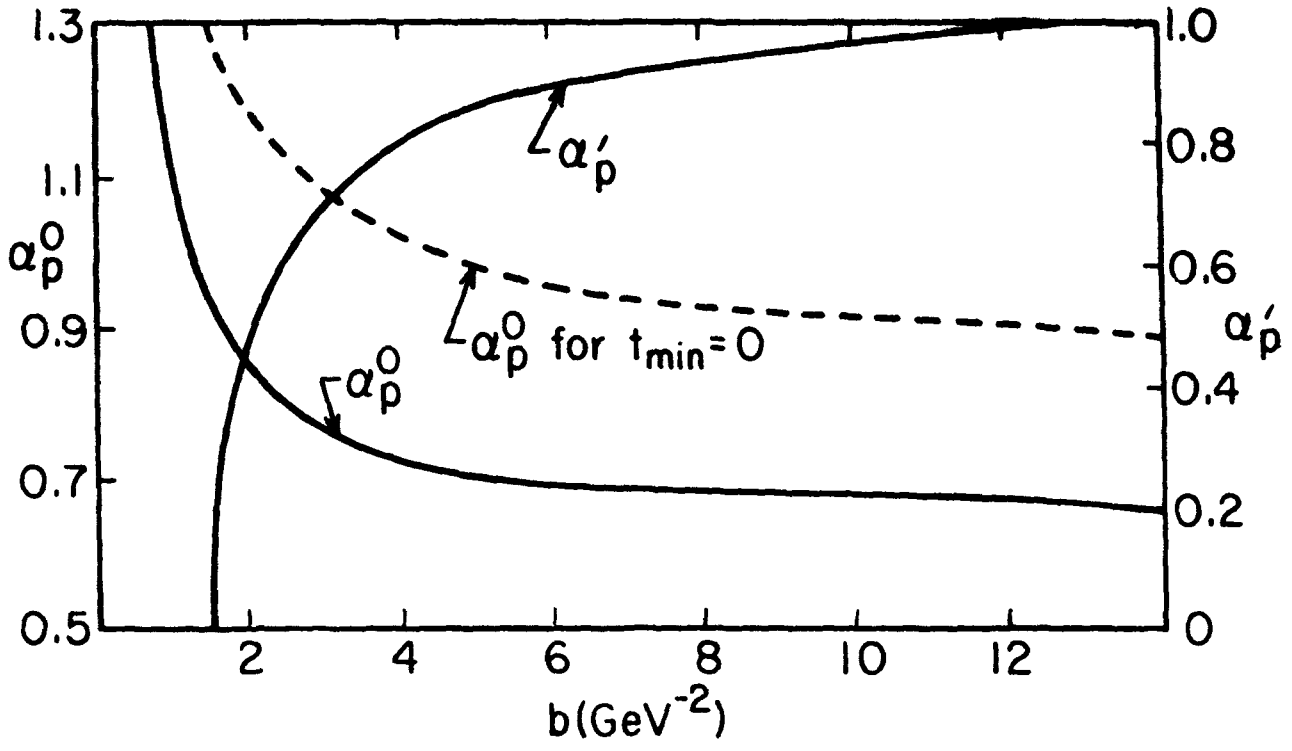
1.3
1.1
0.9
0.7
0.5
α_p^0
1.0
0.8
0.6
0.4
0.2
0
α'_p
α'_p
α_p^0 for $t_{min}=0$
α_p^0
2
4
6
8
10
12
b(GeV^{-2})

Fig. 5a

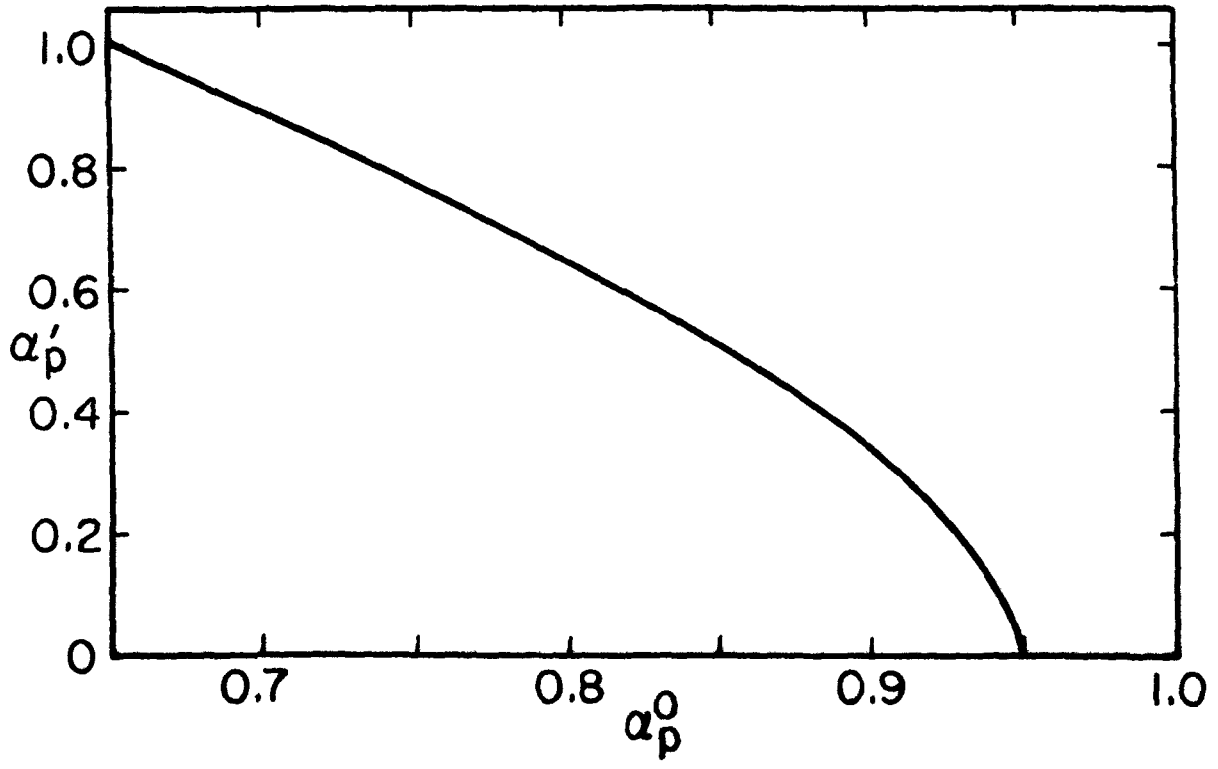
1.0
0.8
0.6
0.4
0.2
0
α'_p
0.7
0.8
0.9
1.0
α_p^0

Fig. 5b

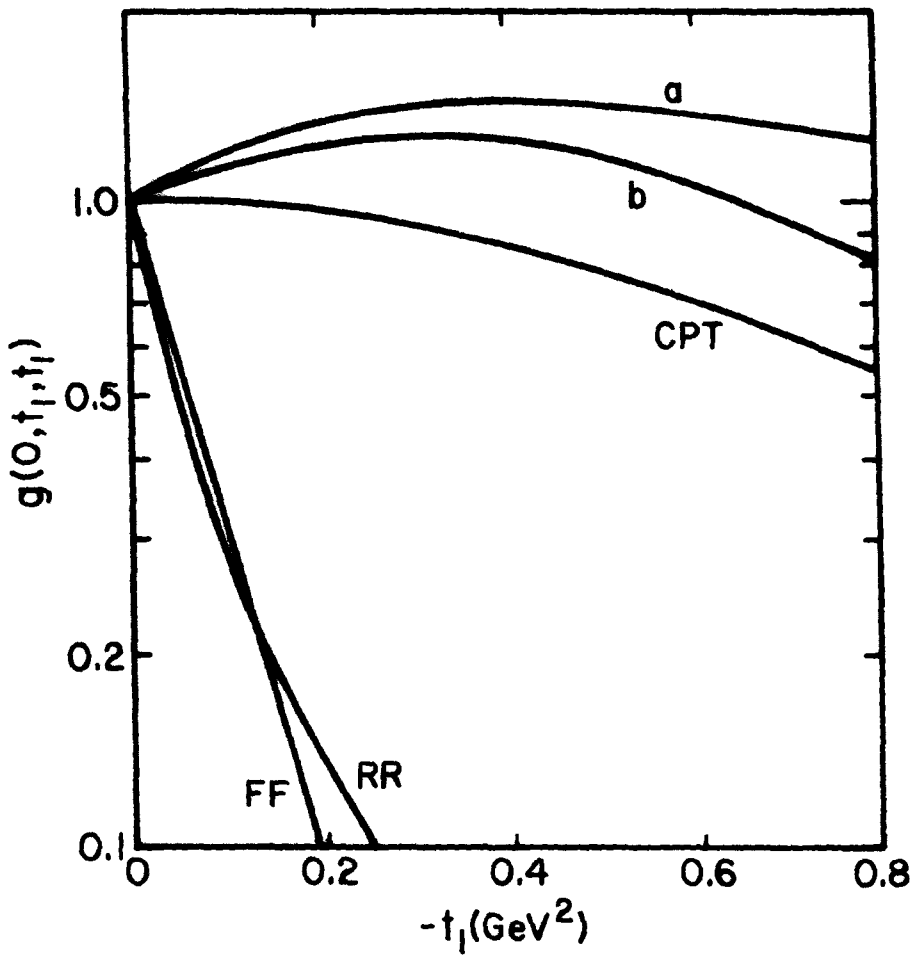

Fig. 5c

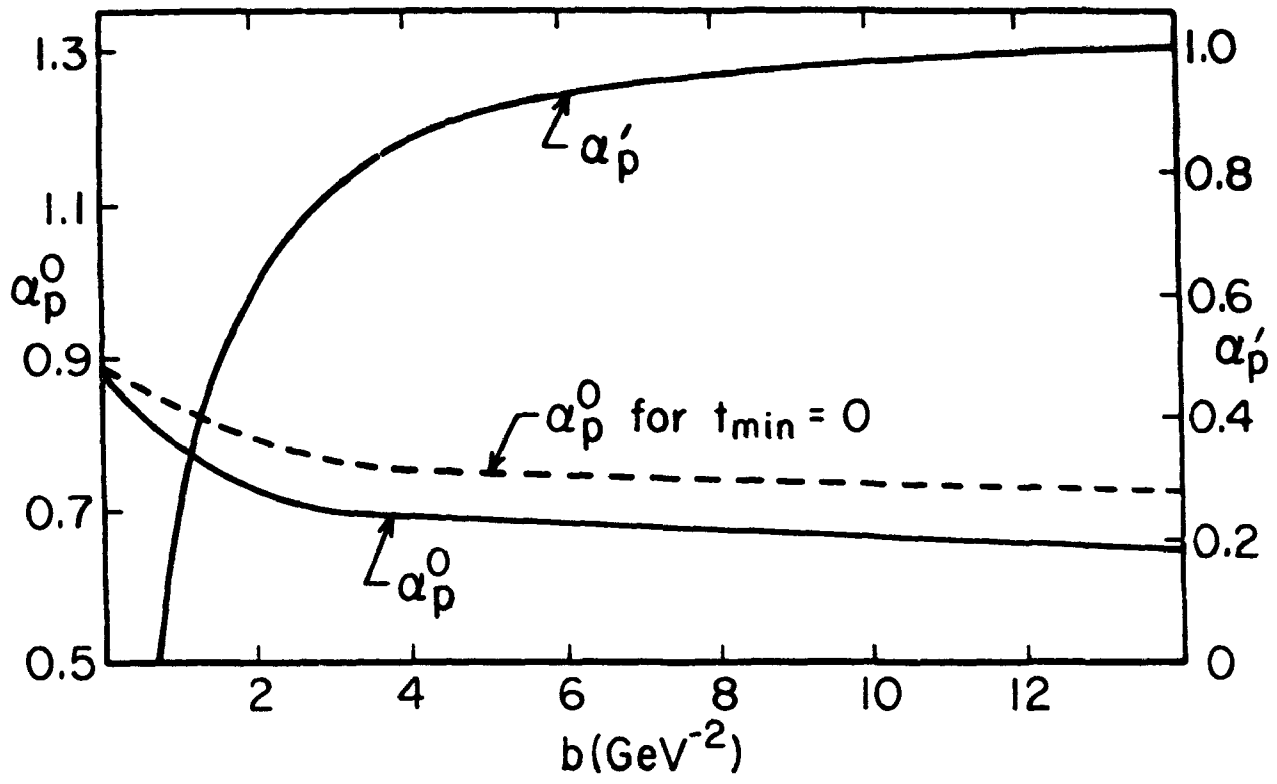
1.3
1.1
0.9
0.7
0.5
α_p^0
1.0
0.8
0.6
0.4
0.2
0
α_p'
α_p'
α_p^0 for $t_{min} = 0$
α_p^0
2
4
6
8
10
12
b(GeV^{-2})

Fig. 6a

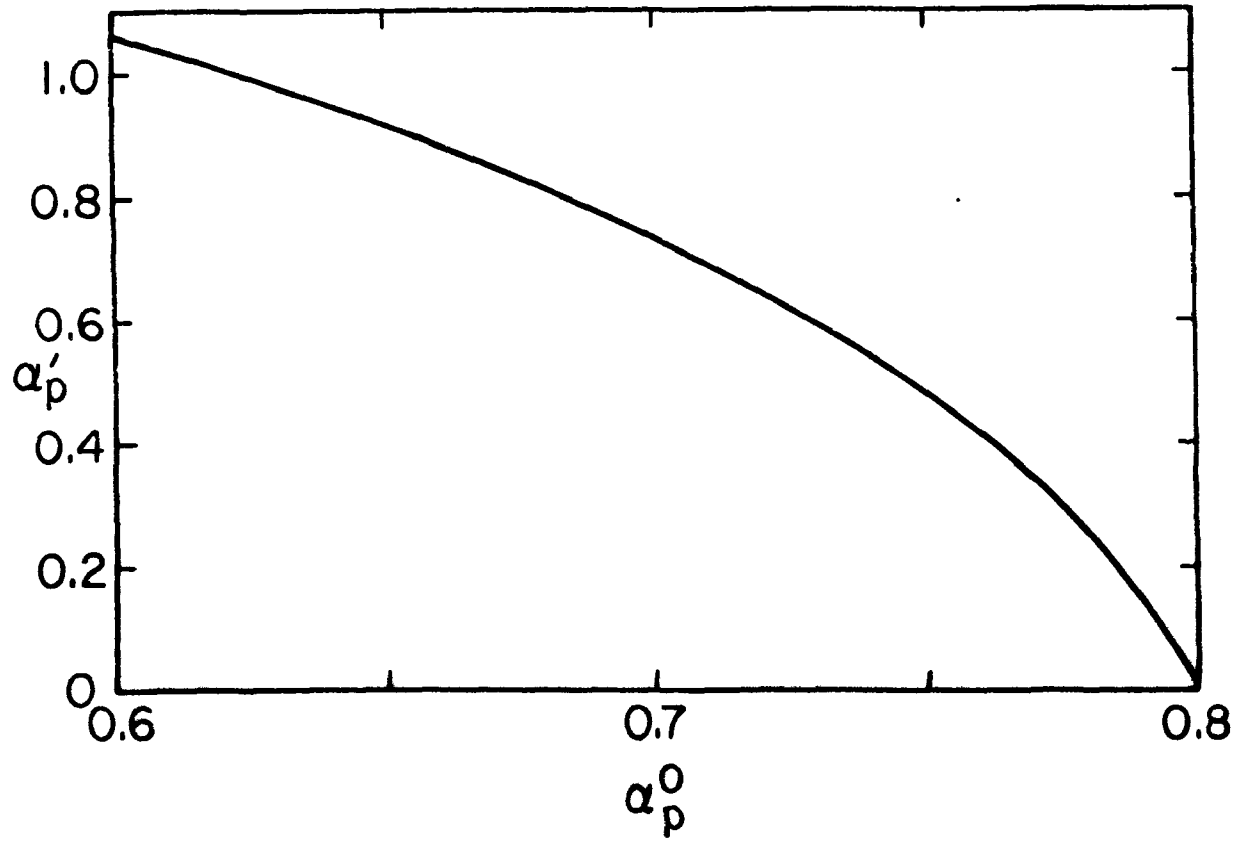
1.0
0.8
0.6
0.4
0.2
0
α_p'
0.6
0.7
0.8
α_p^0

Fig. 6b

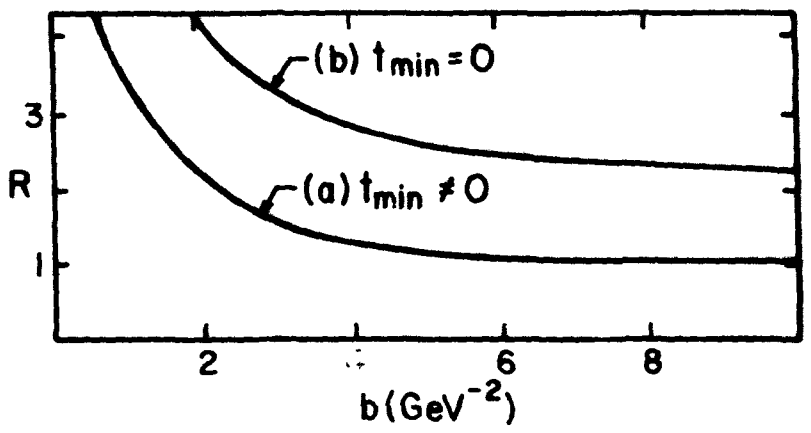

Fig. 7

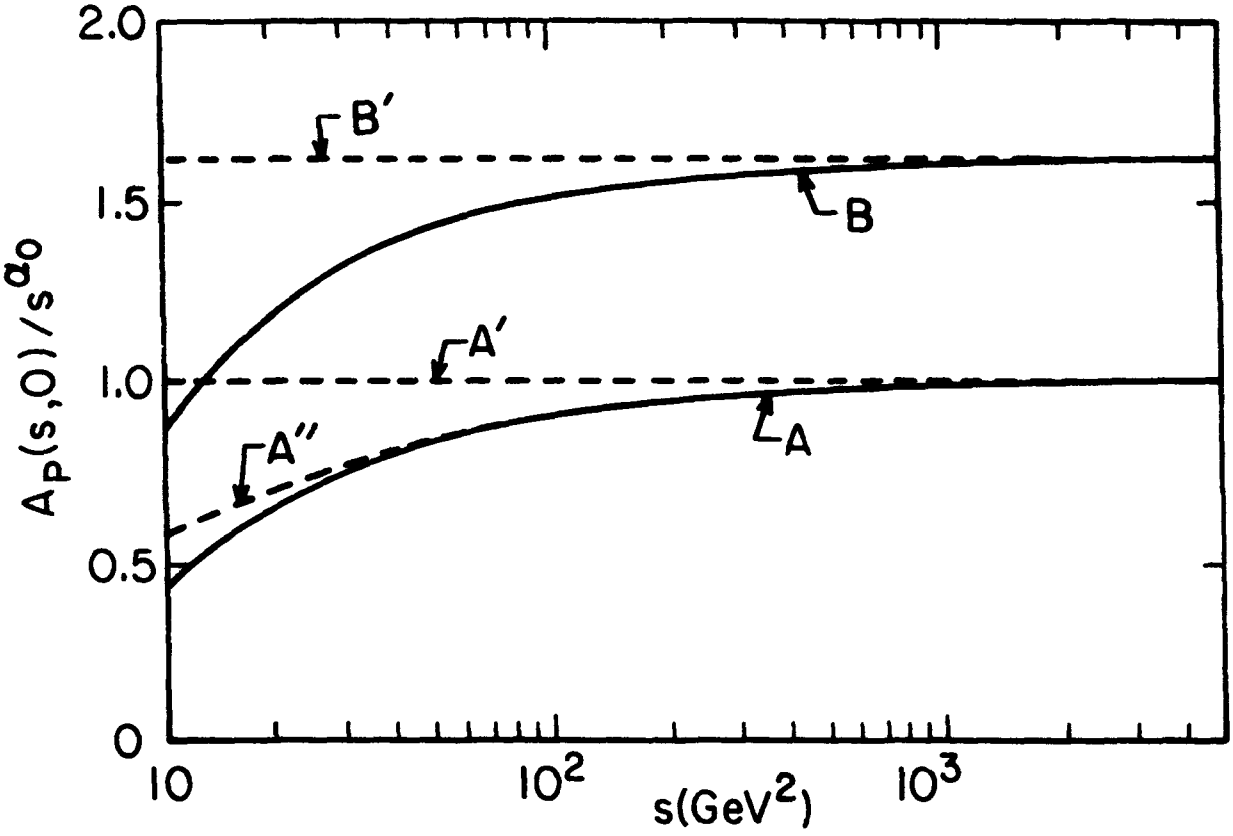
2.0
1.5
1.0
0.5
0
B′
B
A′
A″
A
$A_P(s,0)/s^{\alpha_0}$
10
10^2
10^3
s(GeV^2)

Fig. 8

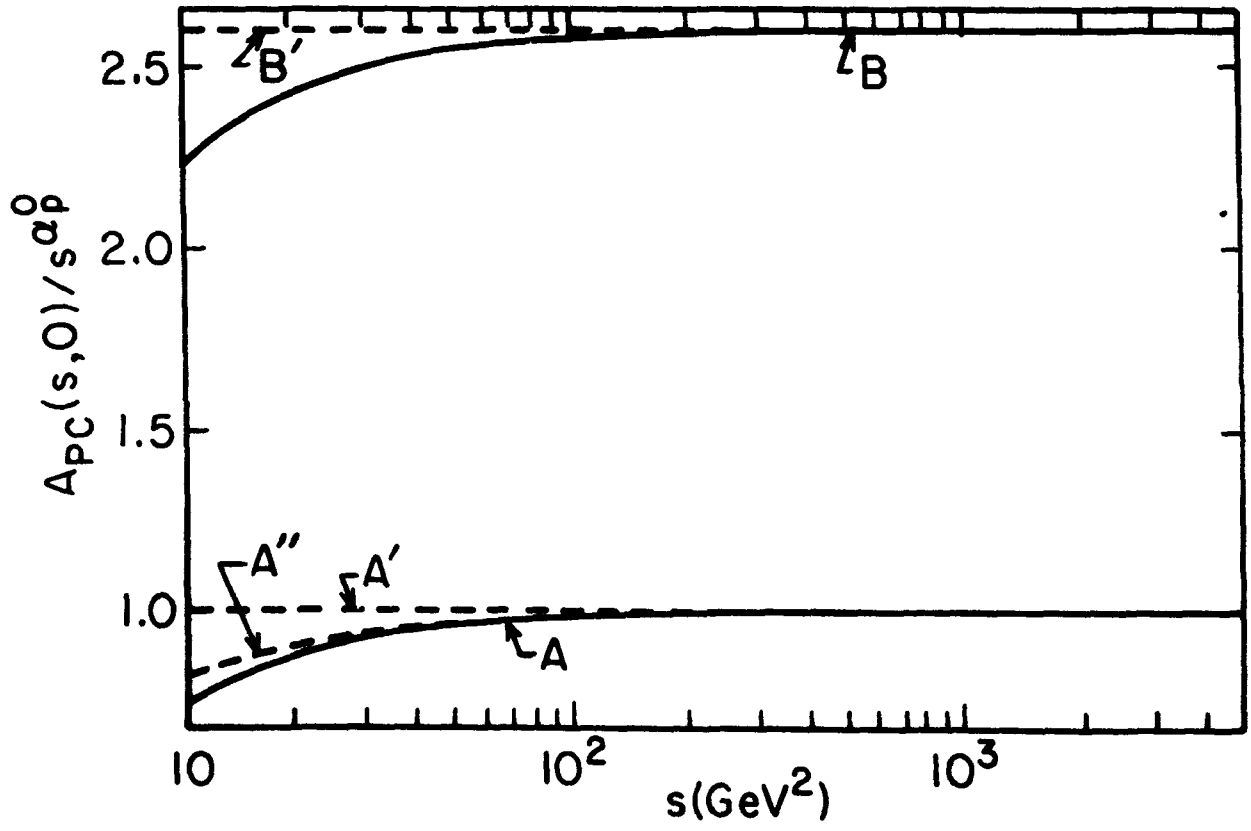
2.5
2.0
1.5
1.0
B′
B
A″
A′
A
$A_{PC}(s,0)/s^{\alpha_P^0}$
10
10^2
10^3
s(GeV^2)

Fig. 9

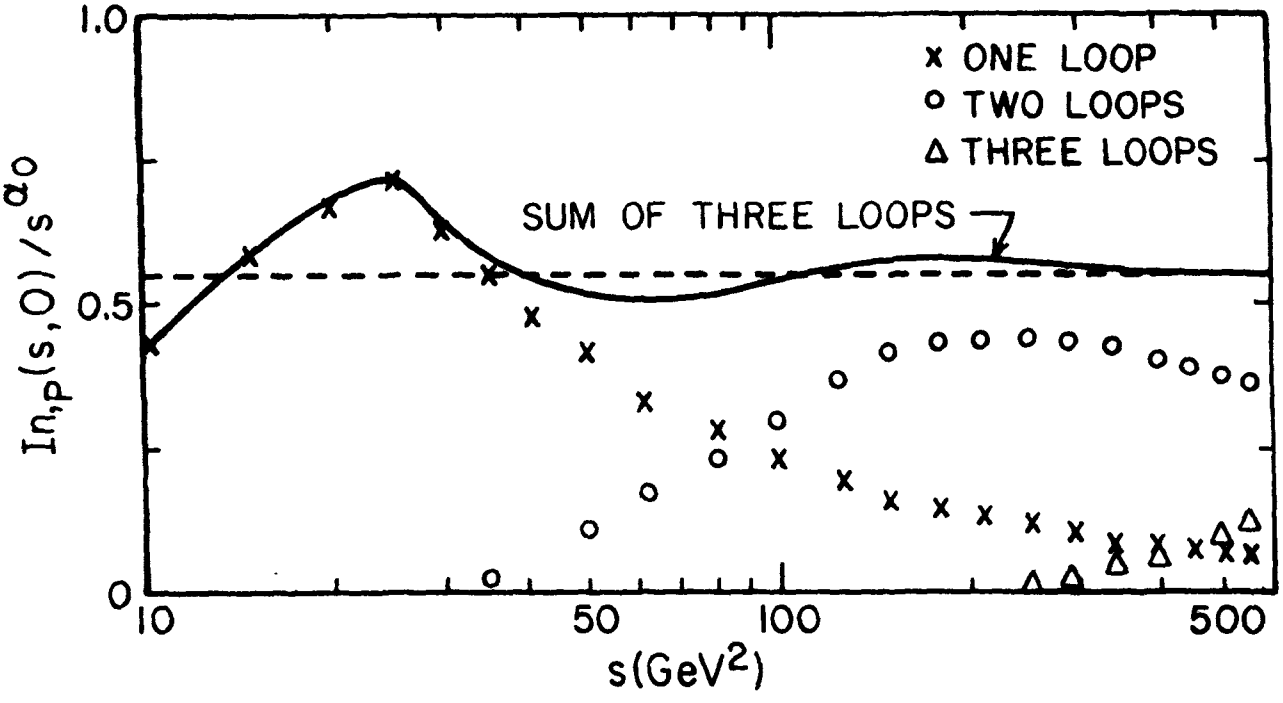
1.0
0.5
0
10
50
100
500
s(GeV²)
Im,P(s,0)/s^α0
x ONE LOOP
o TWO LOOPS
Δ THREE LOOPS
SUM OF THREE LOOPS

Fig. 10

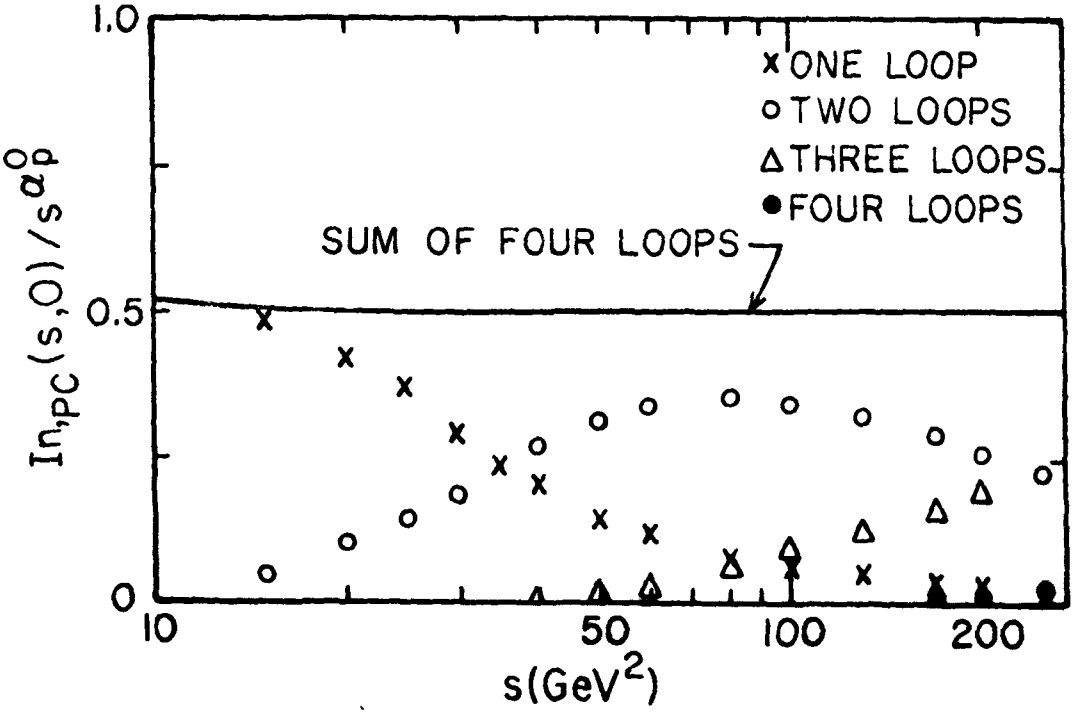
1.0
0.5
0
10
50
100
200
s(GeV²)
Im,PC(s,0)/s^α0_P
x ONE LOOP
o TWO LOOPS
Δ THREE LOOPS
● FOUR LOOPS
SUM OF FOUR LOOPS

Fig. 11